Measurement of Global and Regional Left Ventricular Function by Cardiac PET

Tom R. Miller, Jerold W. Wallis, Brian R. Landy, Robert J. Gropler and Chander L. Sabharwal

The Edward Mallinckrodt Institute of Radiology, Washington University School of Medicine, St. Louis, Missouri

To permit assessment by positron tomography of left ventricular mechanical function, methods were developed to measure ejection fraction and regional wall motion and produce realistic images of the beating heart from ECG-gated PET data. **Methods:** Following red cell labeling with ^{15}O-carbon monoxide, seven-slice PET data were collected in list mode and reformatted into 16 time frames. Volume-rendered cine images were created by the depth-weighted maximum-activity method. To determine the left ventricular ejection fraction, background was subtracted in voxels outside the heart and the cubic datasets were rotated to the angle with the best septal separation. Depth weighting was applied to simulate a ^{99m}Tc study, and the beating images were rendered by summing counts along parallel projection rays. These techniques were validated in 16 patients by comparison with planar studies performed with ^{99m}Tc-red cells. **Results:** Visual grading of regional wall motion yielded exact agreement between the PET and ^{99m}Tc methods in 62% of walls with agreement within one grade in 94%. Assessment of quantitative regional wall motion agreed closely with an independent threshold edge detection method. **Conclusion:** PET techniques have been developed to measure left-ventricular ejection fraction and regional wall motion and to produce realistic beating images of the cardiac blood pool. This information can be obtained at the same time as measurements of perfusion and metabolism and in the same spatial orientation, thereby permitting quantitative assessment by positron tomography of global and regional mechanical function in relation to flow and metabolism.

Key Words: PET; left ventricular function; computers

J Nucl Med 1994; 35:999–1005

PET studies of the heart typically focus on evaluation of myocardial blood flow and metabolism. These measurements must frequently be correlated with changes in left ventricular mechanical function, either global or regional, to fully delineate the pathophysiologic process of interest. This is the case in left ventricular myocardial segments displaying systolic dysfunction where the preservation of glucose metabolism or overall oxidative metabolism are markers of jeopardized but still viable myocardium in patients with coronary artery disease (CAD) (*1,2*). Typically, this comparison requires measurement of mechanical function using a different imaging modality such as echocardiography, radionuclide ventriculography or MRI. Unfortunately, this information may be obtained at a different time from the PET studies, and the images may be produced in planes different from those obtained using PET, thus leading to errors in registration of anatomic regions between the different modalities.

Here we describe methods to measure left ventricular ejection fraction and regional wall motion and produce a realistic image of the beating heart from ECG-gated PET data following red cell labeling with ^{15}O-carbon monoxide. This information can be obtained immediately before or after other measurements of perfusion and metabolism and in the same spatial orientation. Consequently, the confounding issues due to differing loading conditions or physiology between the measurements of perfusion, metabolism and function are reduced, and misregistration of the images is eliminated. The PET methods were validated by comparison with measurements of global and regional function using conventional ECG-gated blood-pool imaging using ^{99m}Tc-labeled red blood cells.

METHODS

Patients

Sixteen patients (14 males, 2 females, age range 39–68 yr) underwent ECG-gated PET imaging employing ^{15}O-carbon monoxide-labeled red blood cells and were all being evaluated clinically for CAD. These patients also had conventional gated blood-pool imaging using ^{99m}Tc-labeled red blood cells within 24 hr of the PET studies. Fourteen had evidence of myocardial infarction. Eight had undergone coronary bypass grafting, and balloon angioplasty had been performed in four.

Instrumentation, Radiopharmaceuticals and Data Acquisition

Images were obtained using the SP-3000-E (PETT Electronics, Inc., St. Louis, MO), a seven-slice PET tomograph with slice spacing of 14.2 mm and transaxial spatial resolution of 8.5 mm FWHM. After a transmission scan, data were acquired in list-mode for 5 min following inhalation of 40 mCi of ^{15}O-carbon monoxide to label the patient's red blood cells. Following correction for attenuation, the ECG-gated data were reconstructed at a 10-mm Gaussian resolution into 16 time frames per R-R interval with each frame consisting of seven 160 × 160-pixel transaxial images with pixel dimension of 3.1 × 3.1 mm^2. To speed process-

Received Sept. 14, 1993; revision accepted Feb. 10, 1994.

For correspondence or reprints contact: Tom R. Miller, MD, PhD, The Edward Mallinckrodt Institute of Radiology, 510 S. Kingshighway Blvd., St. Louis, MO 63110.

ing, the 64 × 64-pixel region centered on the heart was selected for subsequent analysis.

Planar gated blood-pool imaging was performed following conventional clinical methods. Images were collected on a standard field-of-view scintillation camera equipped with a low-energy all-purpose parallel-hole collimator. The patients' red blood cells were labeled by the in vivo method with 25 mCi of ^{99m}Tc. Data were collected in the best septal orientation with a 10 to 15-degree caudal tilt and in projections 45 degrees more anteriorly and more posteriorly. Images in each projection were acquired for a total of 7-million counts in a 64 × 64-pixel matrix with 32 frames per R-R interval.

Data Analysis

Interpolation and Filtering. For each time frame of the PET studies, tri-linear interpolation was applied to the 64 × 64 × 7 data to yield a three-dimensional image with equal voxel dimensions. The cranial and caudal ends of the data were padded with zeros to yield 16 cubic data sets of 64 × 64 × 64 voxels. Following techniques developed by our group (*3,4*), a three-dimensional Wiener filter was applied with a cutoff frequency of 0.12 cycles/pixel, and temporal low-pass filtering was performed to yield images with an acceptable signal-to-noise ratio. A similar filter was applied to the planar ^{99m}Tc data.

Volume-rendered Cine Display. Volume rendering of the PET data was performed by the depth-weighted maximum-activity method as we previously described for SPECT (*5,6*), including gated-SPECT blood-pool imaging (*7*). A realistic cine display of the beating heart was produced that can be viewed at multiple interactively selected angles.

Left Ventricular Ejection Fraction. The left ventricular ejection fraction (LVEF) was determined for the PET data by the ratio of counts within the ventricle at end-diastole and end-systole, LVEF = (EDC − ESC)/EDC, where EDC and ESC are the total background-subtracted left-ventricular counts at end-diastole and end-systole, respectively. This method parallels the technique routinely employed in conventional planar imaging with ^{99m}Tc. A fast, simple approach was employed in which the data were reduced to a two-dimensional form to closely mimic a conventional gated blood-pool study obtained with ^{99m}Tc. The ejection fraction was then determined with clinical two-dimensional software. The following steps were followed:

1. The angle best separating the two ventricles was selected by viewing the volume-rendered cine display, and each cubic dataset was rotated to this angle with a 12-degree caudal tilt applied to partially separate the left atrium and left ventricle.
2. Background activity outside the cardiac blood pool was eliminated by zeroing the activity in all voxels with counts less than 35% of the peak blood-pool counts. Count profiles through the center of the left ventricle were evaluated in several patients with this threshold value chosen to leave only a small amount of extra-cardiac activity while leaving all voxels within the heart undisturbed. Analysis with an alternate choice of 20% led to only minimal change in the ejection fractions.
3. Depth-dependent attenuation was applied to simulate a ^{99m}Tc study by reducing the counts in each voxel according to the distance from the rotated front face of the cube employing a linear attenuation coefficient of 0.13/cm. Each cube was then rendered into a two-dimensional image by summing the counts in all voxels along each projection ray.

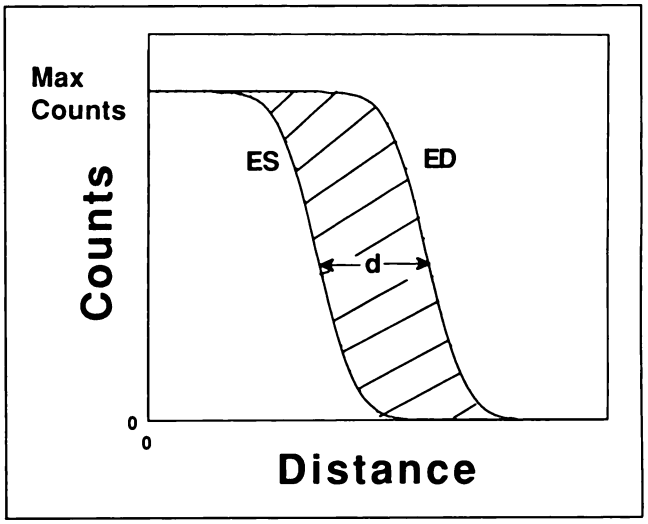

FIGURE 1. Motion of the cardiac blood pool is shown for a simplified one-dimensional case with the endocardial border shown at end-systole (ES) and end-diastole (ED). The distance moved, d, is equal to the shaded area between the ED and ES borders (RayCounts in Equation 1) divided by the counts at the center of the ventricle, MaxCounts.

4. The ejection fraction was determined with use of the same program as employed for conventional ^{99m}Tc imaging, as described below, except without background subtraction.

Quantitative Regional Wall Motion. Left-ventricular regional wall motion was quantified in the PET studies by a method related to the stroke and paradox images employed in planar blood-pool imaging with ^{99m}Tc (*8*). First, the 64^3-pixel three-dimensional images at end-diastole and end-systole were obliquely rotated to align the long axis of the left ventricle along the z-axis following methods employed in SPECT myocardial imaging (*9,10*). For each dataset, a region of interest (ROI) was then manually drawn about the left ventricle on the central short-axis slice. Voxels outside this region in all short-axis slices were set to a value of zero. The cube was then rotated to the horizontal long-axis position with another ROI drawn about the ventricle with zeroing of voxels outside the region. The cubes were then rotated to the vertical long-axis position and the process was repeated. The left ventricle was thus isolated as the intersection of the manually-defined regions in the three orthogonal planes. A new cubic dataset was created by subtracting the counts in every voxel in the end-systolic cube from the counts in the corresponding voxel in the end-diastolic cube. Both positive and negative values were retained in the new "wall motion" cube. The resulting data represent the three-dimensional analog of the "stroke" and "paradox" images in planar imaging. Thus, this wall motion cube contains only a shell of data around the left ventricle with positive values for inward systolic motion and negative values for paradoxical motion.

Along any given ray passing perpendicular to the ventricular wall, the motion of that wall can be obtained by integrating the activity in the wall motion cube (see Fig. 1 for a simplified one-dimensional case). The distance the wall moves between end-diastole and end-systole, d, is obtained in three dimensions from the formula

$$d\ (mm) = RayCounts/MaxCounts. \qquad Eq.\ 1$$

RayCounts is the total counts along the searching ray (the shaded area in Fig. 1), and MaxCounts is the activity in 1 mm^3 of blood at the center of the left ventricle. We observed a 5%–10% reduction in maximum counts at end-systole in a few patients with small end-systolic dimensions due to the partial volume effect. Thus, the end-systolic data were scaled to have equal maximum counts as the end-diastolic data before the wall-motion cube was produced.

A polar bull's-eye display of regional wall motion, analogous to the familiar bull's eye display employed in clinical myocardial imaging (*9,10*), can then be obtained in the following way. While viewing the short- and long-axis blood-pool images, an ellipsoidal-shaped boundary was manually placed around the margin of the ventricular blood pool. The ellipsoid can be represented mathematically in Cartesian coordinates by the equation

$$x = x_c + a \cos \phi \sin \theta,$$
$$y = y_c + b \sin \phi \sin \theta, \qquad \text{Eq. 2}$$
$$z = z_c + c \cos \theta,$$

where (x_c, y_c, z_c) is the ellipsoid center, a = b is the semi-minor axis, c is the semi-major axis, and the angles θ and ϕ are analogous to the latitude and longitude coordinates in a cartographic representation of the earth or the radial and tangential coordinates in the bull's-eye display. Searching rays were generated perpendicular to the myocardial boundary at each angle in 1.4-degree increments with the values for wall motion placed in the corresponding locations in the bull's-eye. Regions with positive wall motion are shown in a stroke bull's-eye and those with negative values in a paradox bull's-eye.

This method involves selection of only single time points for end-diastole and for end-systole. Thus, regional wall motion will be underestimated in some cases because of the variable contraction times of different segments of the ventricle. The small changes in phase angle across the ventricle that are typically observed in conventional phase analysis of planar studies suggest that this effect will usually be small. In some patients, e.g., those with aneurysms, different end-diastole and end-systole points could be selected if needed.

Planar Gated Blood Pool Studies. The left ventricular ejection fraction was determined in the same way for the ^{99m}Tc gated blood pool studies and the two-dimensionally rendered PET studies employing standard clinical software (*11*) with manually defined end-diastolic and end-systolic regions and a background region lateral to the left ventricle.

Validation

Ejection Fraction. The left-ventricular ejection fractions obtained by the PET and planar ^{99m}Tc methods were graphed and fitted by linear least-squares regression. Intra- and interobserver variability was assessed by repeat computation of ejection fractions by two observers. The results are quantified by the correlation coefficient, r, and the standard error of the estimate, see, also called the RMS residual.

Regional Wall Motion. To assess the accuracy of the volume-rendered cine display, particularly in evaluation of ventricular wall motion, three physicians experienced in the interpretation of cardiac blood-pool studies visually graded the left ventricular wall motion from the beating cine displays for the PET and the three-view ^{99m}Tc studies in the 16 patients. Seven walls (anterolateral, lateral, septal, anteroseptal, inferior, posterior and apical) were graded on a scale of 1 (normal) to 5 (aneurysmal). The PET and ^{99m}Tc studies were viewed in random order and a consensus wall motion score was used for each study. Agreement between the imaging methods was quantified as the number of walls with near and complete agreement.

The quantitative PET measurement of regional wall motion was evaluated by comparison with the wall motion determined from the same data by a completely different method: measurement of wall motion by edge detection at end-diastole and end-systole. The blood-pool boundaries were determined from the cubic data by a simple thresholding algorithm after isolation of the left ventricle. The boundary of the blood pool was chosen at 40% of the counts in the voxel at the center of the left ventricle. This value was determined by visual inspection of count profiles in several studies; evaluation with a 50% threshold did not significantly alter the correlation coefficient comparing the two methods. Linear interpolation was employed between integer voxel positions below and above the threshold to give the wall location at the threshold value for fractional voxel positions. The distance between the end-diastolic and end-systolic blood-pool margins was computed from the mid-ventricular short-axis slices at the anterior, lateral, septal and inferior positions and from the horizontal long-axis slice at the apex. The wall motion by the stroke and edge detection methods was graphed for these five positions in the 16 patients, and the data were fitted by linear regression.

Computer Processing

Reconstruction of the list-mode data into transaxial slices consumed approximately 90 min. The reformatting of the seven-slice PET data into cubic form and the digital filtering required approximately 7 min on a modern RISC workstation (DECstation 5000/200, Digital Equipment Corp., Maynard, MA). Volume rendering to produce the cine display required an additional 12 min. Calculation of the ejection fraction required 5 min. Generation of the wall-motion images required approximately 12 min. Thus, after reconstruction of the list-mode data, a study could be completely processed in approximately 35 min.

RESULTS

Cine Display

PET images from the beating cine display of a patient with a large antero-apical myocardial infarction extending into the inferior wall are shown in Figure 2. Note the akinetic region at the apex extending into the adjacent anterior and inferior walls and good wall motion in the postero-inferior and antero-basal regions. The left atrium is well seen on the lateral view.

Ejection Fraction

Figure 3 shows the ejection fraction results obtained from the planar ^{99m}Tc and PET studies (y = 0.900x + 3.686, r = 0.96, see = 5.80%). Figure 4 shows two determinations of the ejection fraction from the PET study obtained by one observer (intraobserver variability) (y = 0.992x + 0.256, r = 0.99, see = 3.36%), while Figure 5 compares the PET results for two observers (interobserver variability) (y = 0.953x + 1.646, r = 0.98, see = 3.32%).

Regional Wall Motion

The visual grading of wall motion from the cine display for the seven walls in the 16 patients was performed for all

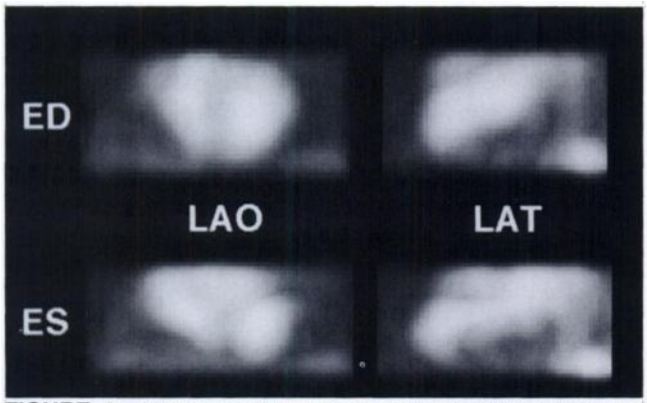

FIGURE 2. Volume-rendered images at end-diastole (ED) and end-systole (ES) are shown in the left anterior oblique (LAO) and left lateral (LAT) projections in a patient with antero-apical myocardial infarction.

but four walls at the inferior margin of the PET images. This analysis in 108 walls yielded exact agreement between the planar and PET studies in 67 (62%) and agreement within one grade in 102 (94%) with only six walls (6%) differing by two grades.

In Figure 6 a stroke bull's-eye image is shown for the same patient as in Figure 2. Note the poor wall motion centered at the apex and in the septum with good motion more basally and laterally. Figure 7 shows the results for regional wall motion obtained by the wall-motion cube and by the edge detection methods ($y = 0.793x + 0.146$, $r = 0.86$, see = 2.01 mm). Note the good agreement between the two methods of analyzing the PET data. While a true validation by a completely different imaging technique was not performed, the agreement between fundamentally different approaches to determination of wall motion applied to the same data suggests the accuracy of the new method.

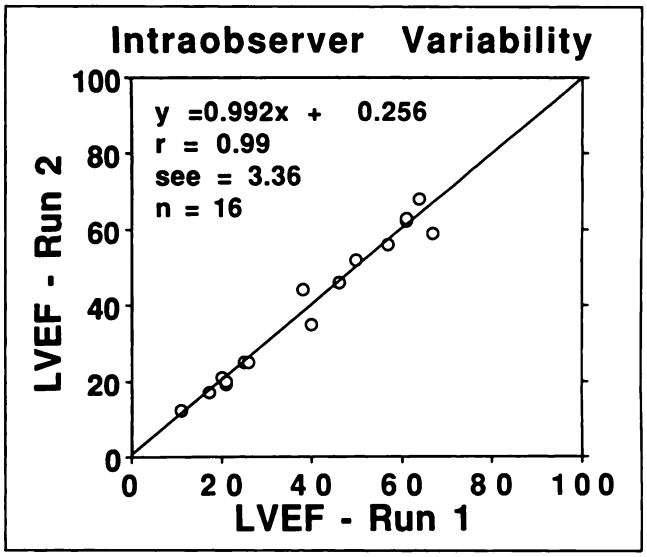

FIGURE 4. Intraobserver variability in ejection fraction determination is shown for repeated processing of the PET ejection fraction data by one observer.

DISCUSSION

PET is a highly developed tool for study of the heart, yielding accurate measurements of myocardial blood flow and quantitative evaluation of biochemistry with tracers such as ^{11}C-acetate and ^{18}F-fluorodeoxyglucose. In contrast to the research with flow and metabolism, little effort has been devoted to assessment of myocardial mechanical function by PET (*12*), possibly because evaluation of ventricular contraction requires ECG gating, thereby imposing additional demands on the instrumentation and, especially, on the computer. Thus, measurement of myocardial contractility has usually been performed by echocardiography, radionuclide ventriculography or contrast ventriculography. This use of different imaging modalities increases the

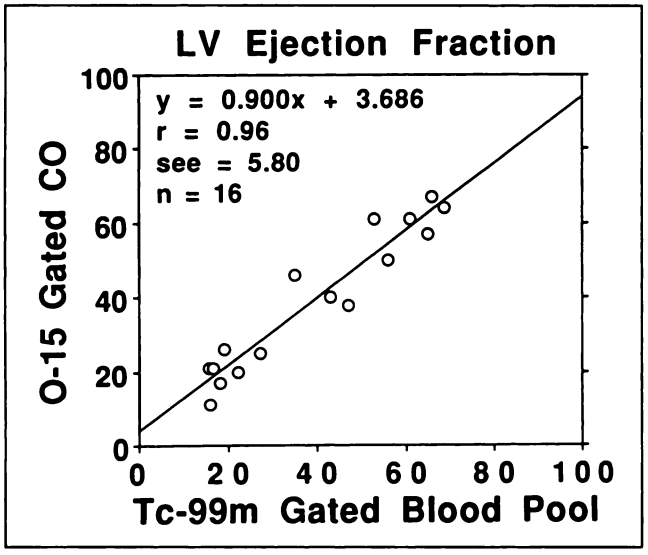

FIGURE 3. The ejection fraction is shown by the conventional ^{99m}Tc method and by PET using ^{15}O-carbon monoxide.

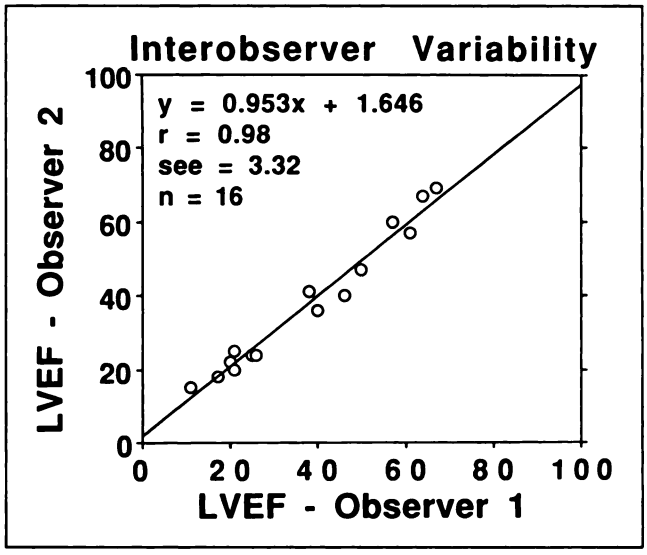

FIGURE 5. Interobserver variability is shown for processing of the PET data by two observers.

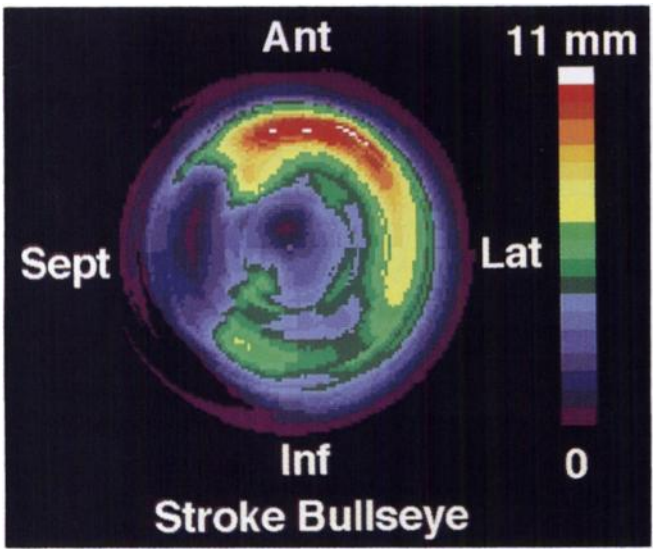

FIGURE 6. The stroke bull's-eye is shown for the same patient as in Figure 2. The maximum value of the color scale represents a motion of 11 mm.

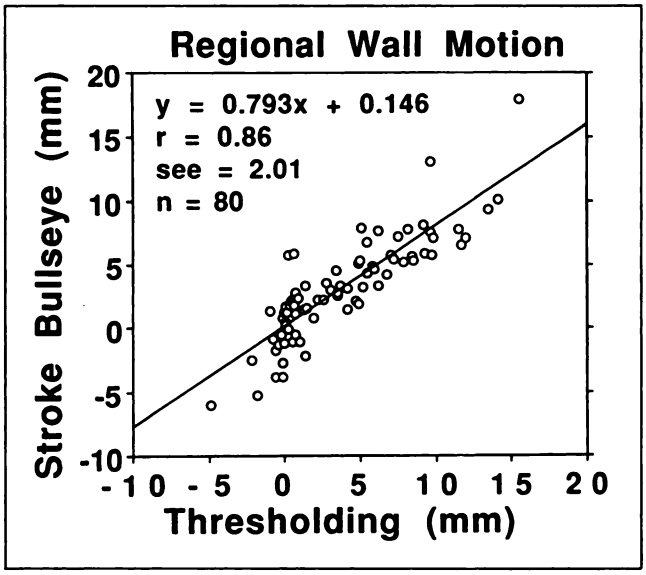

FIGURE 7. Regional wall motion is shown for the thresholding edge-detection method and for the stroke bull's-eye.

complexity of the studies and may result in altered physiology due to time differences while rendering problematic the accurate registration of anatomic segments from images acquired in different planes. The approach described here addresses these deficiencies with use of the readily available blood-pool tracer ^{15}O-carbon monoxide. Computationally tractable methods are presented that yield accurate measurements of global and regional left-ventricular function that are spatially registered with PET studies of flow and metabolism obtained at the same time.

The first step in evaluation of contractile function is visual inspection of the gated images during cine display to assess chamber size and regional wall motion. Our validation studies confirmed the accuracy of the volume-rendering method. This approach provides a more complete qualitative impression of all four cardiac chambers than either echocardiography or cardiac catheterization.

Ejection fraction can be determined by two fundamentally different methods. One method widely employed in ^{99m}Tc SPECT studies involves voxel counting within the left ventricle at end-diastole and end-systole (*13–18*). The ratio of voxels then gives the ejection fraction. We chose to use the other count-based method that follows clinical practice in planar ^{99m}Tc imaging but has been infrequently employed in SPECT studies (*19*). Because detected counts are proportional to chamber volume, the ejection fraction is determined as a count ratio, not a volume (voxel) ratio. This method substantially relaxes the demand on the ventricular edge detector: a somewhat loose, approximate definition of the ventricular boundary is adequate because activity outside the ventricle is minimal, especially after background subtraction or thresholding. Our quantitative assessment of regional wall motion also differs from that of other workers who have relied on edge detection of the blood pool at end-diastole and end-systole (*16,18,20,21*). Integration of total stroke counts, as we have developed, does not require accurate edge detection.

These count-based methods are subject to error due to the partial volume effect (*22,23*). Small ventricles, particularly those at end-systole in patients with high ejection fractions, may have a diameter close to the resolution of the imaging system, thus leading to a reduction in detected counts. This effect will be less pronounced with PET than with SPECT because of the superior spatial resolution of PET. No correction was applied to the ejection fraction calculation; indeed, the partial volume effect is similar or worse for the planar ^{99m}Tc studies with which the PET data

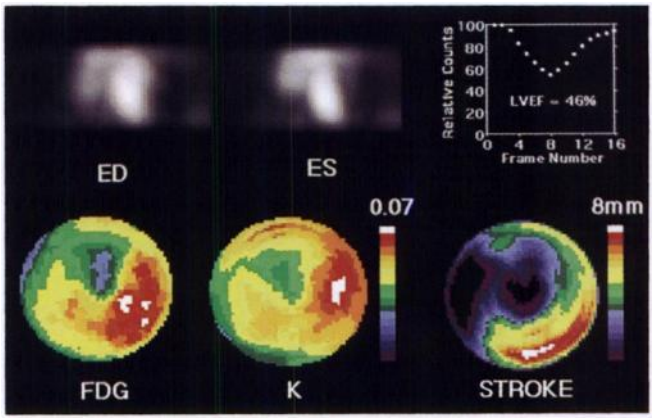

FIGURE 8. Images from a myocardial viability study are shown for a patient with anterior wall myocardial infarction. The top row shows the volume rendered images at end-diastole and end-systole and the ventricular time-activity curve and ejection fraction. The lower left image is a bull's-eye display of glucose metabolism from the FDG study. The center bull's-eye displays the first-order rate constant of acetate clearance, k_1, reflecting regional oxygen consumption, here with a maximum value of 0.07/min. The wall motion image of regional contractile function is on the lower right with a maximum wall motion of 8 mm.

are compared. In the wall motion analysis, the end-systolic data were scaled to have equal maximum counts as the end-diastolic data. We evaluated this partial volume issue further for assessment of wall motion by a one-dimensional computer simulation of ventricular wall motion with ventricles of various sizes imaged over a wide range of spatial resolutions, finding accurate wall motion assessment in all cases.

Initial development of the ejection fraction method involved complete utilization of the three-dimensional nature of the PET data and accurate correction for depth-dependent attenuation. Two problems were encountered with this approach. First, computation time was long, requiring 15–30 min of processing and operator interaction to rotate and render the cubic data and draw the regions in multiple projections. The second difficulty was more serious: the inter- and intraobserver errors were large, probably due to difficulty in specifying the mitral valve plane. This unexpected situation arose because, in contrast to the SPECT case, the left atrium was as intense as the left ventricle after attenuation compensation and because of the complex motion of the mitral valve plane on long-axis images with significant overlap between atrium and ventricle. Thus, the simpler and faster approach described above was adopted in which the PET data were made to resemble a conventional planar study, thereby reducing processing time and attenuating the left atrium. This method is simple and fast and gave accurate, reproducible results.

The absence of a true gold standard for LVEF led us to choose the ^{99m}Tc gated blood-pool study as the standard for comparison. We recognize the limitations inherent in this choice, particularly the underestimation of ejection fraction in large, poorly contracting ventricles caused by gamma-ray attenuation of the posterior activity (*24*). The same limitation is present in our simple method of processing the PET data. We chose to apply attenuation to the PET data because the reduction in left atrial activity greatly facilitated identification of the basal portion of the ventricle, thereby reducing variability in ejection fraction determination, as discussed above for the fully three-dimensional case. Further effort with the three-dimensional, attenuation-free method is in order, perhaps with validation against biplane angiography or gated MRI.

Other workers have developed functional images of regional wall motion. Honda et al. (*25*) derived a bull's-eye image from a stroke cube using gated SPECT with ^{99m}Tc. Their bull's-eye was qualitative in nature because the maximum pixel, rather than the total counts, was selected along each ray. Yamashita et al. (*21*) produced three-dimensional images of wall shortening and phase images of shortening. Others have developed functional images by phase analysis (*26,27*). We also generated phase images, finding them to correspond qualitatively with the quantitative stroke bull's-eyes.

To illustrate integration of the new blood-pool information with studies of metabolism, images are shown in Figure 8 of a 51-yr-old male with recent anterior wall myocardial infarction treated with intravenous thrombolytic agents. Coronary angiography revealed a high-grade proximal stenosis of the left anterior descending coronary artery. He underwent an evaluation of myocardial viability employing ^{15}O-carbon monoxide, ^{18}F-fluorodeoxyglucose to measure glucose metabolism and ^{11}C-acetate to assess oxidative metabolism (*1,2*). Conventional methods were used to generate a bull's-eye display from the FDG transaxial slices (*10*). A bull's-eye display of regional oxygen consumption was obtained from sequential ^{11}C-acetate data with voxel-by-voxel fitting to yield a functional image of the first-order rate constant of acetate clearance, k_1 (*28*). The PET measurement of regional wall motion reveals abnormal wall motion of the septal, anterior and apical walls confirmed by echocardiography. Glucose utilization and oxygen consumption are preserved in most of the territory of the diseased artery displaying abnormal wall motion, thus indicating poorly contracting but viable myocardium except in the apical and antero-apical regions where the glucose and acetate values are low, consistent with nonviable tissue.

CONCLUSION

We present techniques employing ECG-gated PET with ^{15}O-carbon monoxide to measure left ventricular ejection fraction and regional wall motion and to produce realistic beating images of the cardiac blood pool. These methods will facilitate the integration of measurements of myocardial perfusion, metabolism and mechanical function by PET.

ACKNOWLEDGMENTS

This research was supported by grants HL42884 and HL13851 from the National Institutes of Health. Dr. Gropler is a recipient of a Clinician-Scientist Award from the American Heart Association.

REFERENCES

1. Gropler RJ, Geltman EM, Sobel BE. Clinical application of cardiac positron emission tomography. In: Bergmann SR, Sobel BE, ed. *Positron emission tomography of the heart*. Mount Kisco, NY: Futura Publishing Company, Inc.; 1992:255–292.
2. Gropler RJ, Geltman EM, Sampathkumaran K, et al. Functional recovery after coronary revascularization for chronic coronary artery disease is dependent on maintenance of oxidative metabolism. *J Am Coll Cardiol* 1992; 20:569–577.
3. Miller TR, Sampathkumaran KS. Digital filtering in nuclear medicine. *J Nucl Med* 1982;23:66–72.
4. Miller TR, Wallis JW, Wilson AD. Interactive reconstruction in single-photon tomography. *Eur J Nucl Med* 1989;15:189–193.
5. Wallis JW, Miller TR. Three-dimensional display in nuclear medicine. *IEEE Trans Med Imag* 1989;8:297–303.
6. Wallis JW, Miller TR. Volume rendering in three-dimensional display of SPECT images. *J Nucl Med* 1990;31:1421–1430.
7. Miller TR, Wallis JW, Sampathkumaran KS. Three-dimensional display of gated cardiac blood-pool studies. *J Nucl Med* 1989;30:2036–2041.
8. Maddox DE, Holman BC, Wynne J, et al. The ejection fraction image: a new noninvasive index of regional left ventricular wall motion. *Am J Cardiol* 1978;41:1230–1238.
9. Garcia EV, VanTrain K, Haddahi J. Quantification of rotational thallium-201 myocardial tomography. *J Nucl Med* 1985;26:17–26.
10. Miller TR, Starren JB, Grothe RB. Three-dimensional display of positron emission tomography of the heart. *J Nucl Med* 1988;29:530–537.

11. Biello DR, Sampathkumaran KS, Geltman EM, Britson WA, Scott DJ, Grbac RT. Determination of left ventricular ejection fraction: A new method that requires minimal operator training. *J Nucl Med Technol* 1981;9:77–80.
12. Ter-Pogossian MM, Bergmann SE, Sobel BE. Influence of cardiac and respiratory motion on tomographic reconstructions of the heart: implications for quantitative nuclear cardiology. *J Comput Assist Tomogr* 1982;6: 1148–1155.
13. Bunker SR, Hartshorne MF, Schmidt WP, et al. Left ventricular volume determination from single-photon emission computed tomography. *Am J Radiol* 1985;144:295–298.
14. Stadius ML, Williams DL, Harp G, et al. Left ventricular volume determination using single-photon emission computed tomography. *Am J Cardiol* 1985;55:1185–1191.
15. Corbett JR, Jansen DE, Lewis SE, et al. Tomographic gated blood pool radionuclide ventriculography: analysis of wall motion and left ventricular volumes in patients with coronary artery disease. *J Am Coll Cardiol* 1985; 6:349–358.
16. Gill JB, Moore RH, Tamaki N, et al. Multigated blood-pool tomography: new method for the assessment of left ventricular function. *J Nucl Med* 1986;27:1916–1924.
17. Ziada G, Mohamed MM, Hayat N, et al. Quantitative analysis of cardiac function: comparison of electro-cardiogram dual gated single photon emission tomography, planar radionuclide ventriculogram and contrast ventriculography in the determination of LV volume and ejection fraction. *Eur J Nucl Med* 1987;12:592–597.
18. Faber TL, Akers MS, Peshock RM, Corbett JR. Three-dimensional motion and perfusion quantification in gated single-photon emission computed tomograms. *J Nucl Med* 1991;32:2311–2317.
19. Caputo GR, Graham MM, Brust KD, Kennedy JW, Nelp WB. Measurement of left ventricular volume using single-photon emission computed tomography. *Am J Cardiol* 1985;56:781–786.
20. Barat J, Brendel AJ, Colle J, et al. Quantitative analysis of left-ventricular function using gated single photon emission tomography. *J Nucl Med* 1984; 25:1167–1174.
21. Yamashita K, Tanaka M, Asada N, et al. A new method of three-dimensional analysis of left ventricular wall motion. *Eur J Nucl Med* 1988;14:113–119.
22. Miller TR, Wallis JW, Grothe RA. Design and use of PET tomographs: the effect of slice spacing. *J Nucl Med* 1990;31:1732–1739.
23. Hoffman EJ, Huang S-C, Phelps ME. Quantitation in positron emission tomography: 1. Effect of object size. *J Comput Assist Tomogr* 1979;3:299–308.
24. Schneider RM, Jaszczak RJ, Coleman RE, Cobb FR. Disproportionate effects of regional hypokinesis on radionuclide ejection fraction: compensation using attenuation-corrected ventricular volumes. *J Nucl Med* 1984; 25:747–754.
25. Honda N, Machida K, Mamiya T, et al. Two-dimensional polar display of cardiac blood pool SPECT. *Eur J Nucl Med* 1989;15:133–136.
26. Nakajima K, Bunko H, Tonami N, Tada A, Hisada K. Quantification of segmental wall motion by length-based fourier analysis. *J Nucl Med* 1984; 24:917–921.
27. Mate E, Mester J, Csernay L, Kuba A, Madani S, Makay A. Three-dimensional presentation of the fourier amplitude and phase: a fast display method for gated cardiac blood-pool SPECT. *J Nucl Med* 1992;33: 458–462.
28. Miller TR, Wallis JW, Geltman EM, Bergmann SR. Three-dimensional functional images of myocardial oxygen consumption from positron tomography. *J Nucl Med* 1990;31:2064–2068.

EDITORIAL

Assessment of Mechanical Function as an Adjunct to Myocardial Perfusion/Metabolism Emission Tomography Studies

An increasing number of myocardial perfusion and metabolism studies are being performed with either PET or SPECT to assess myocardial perfusion and viability. To date, the conventional imaging approach has been to perform these studies ungated to expedite image acquisition, processing, interpretation and storage. Unfortunately, ungated acquisition limits the clinical value of the perfusion/metabolism study in an important way. Functional information that may be gathered from the qualitative or quantitative analysis of the motion and thickening of the myocardial wall is lost. The article by Miller et al. (*1*) in this issue describes a method of assessment by PET of left ventricular global and regional mechanical function from ECG-gated images following red cell labeling with ^{15}O-carbon monoxide. Clearly, in these days of health care reforms, fiscally responsible referring physicians would never request that a myocardial perfusion/metabolism emission tomography study be performed on a patient just to assess ventricular function. This assessment is customarily performed adequately and more frugally with other techniques such as radionuclide ventriculography or two-dimensional echocardiography. Nevertheless, the same fiscally-minded referring physicians would want to utilize available functional information when they send their patients for the assessment of myocardial perfusion and/or metabolism using emission tomography studies.

In using ^{15}O-water studies for assessment of myocardial perfusion, a correction is required for the radioactivity in the vascular compartment (*2*). The group at Washington University has used a separate inhalation of ^{15}O-carbon monoxide to label red blood cells and delineate the vascular pool in order to make this correction (*2*). Thus, Miller et al. (*1*) are suggesting that if the ^{15}O-carbon monoxide study has to be performed in order to make this correction, why not capture and quantify the important myocardial mechanical function information that it provides. This assessment of myocardial function is particularly relevant in questions of myocardial viability, since a wall that is moving, and particularly thickening, is viable.

Moreover, as pointed out by Miller et al. (*1*), simultaneous assessment of myocardial function and perfusion/metabolism guarantees accurate registration of anatomic segments between the function and perfusion/metabolism study as well as guaranteeing the assessment of these myocardial characteristics in the same physiologic state. These are two attributes which are very difficult to guarantee when performing the assessment of function and perfusion/metabolism with different modalities at different times. The measurement of global and regional left ventricular function from cardiac

Received Mar. 16, 1994; accepted Mar. 17, 1994.
For correspondence or reprints contact: Ernest V. Garcia, PhD, Center for Positron Emission Tomography, Emory University Hospital, 1364 Clifton Road, NE, Atlanta, GA 30322.